Appears in the Proceedings of IEEE VTC'07, April 2007.

Influence of 3-D Spatial Correlation on the Capacity of MIMO Mobile-to-Mobile Channels

Alenka G. Zajić and Gordon L. Stüber
School of Electrical and Computer Engineering
Georgia Institute of Technology, Atlanta, GA 30332 USA

***Abstract*—A three-dimensional (3-D) theoretical model for MIMO mobile-to-mobile (M-to-M) multipath fading channels is proposed and its spatial correlation function is derived. This correlation function is used to evaluate the effect of spatial correlation on the capacity of uniform linear antenna arrays. The effects of antenna spacing and antenna orientations on capacity are studied.**

I. Introduction

Mobile-to-mobile (M-to-M) channels, where both the transmitter ($\mathrm{T_x}$) and the receiver ($\mathrm{R_x}$) are in motion and equipped with low elevation antennas, find application in mobile ad-hoc wireless networks, intelligent transportation systems, and relay-based cellular networks. To successfully design M-to-M systems, it is necessary to have a detailed knowledge of the multipath fading channel and its statistical properties. Early studies of single-input-single-output (SISO) M-to-M Rayleigh fading channels are reported in [1], [2], wherein a reference model was proposed for SISO M-to-M Rayleigh fading channels. Simulation models for SISO M-to-M channels have been proposed in [3]-[5]. Recently, reference models for narrow-band multiple-input-multiple-output (MIMO) M-to-M channels have been proposed in [6], [7]. Simulation models for MIMO M-to-M channels have been proposed in [8], [9].

A common feature of the above models is that the incident waves are assumed to travel horizontally, i.e. they are two-dimensional (2-D) models. For conventional fixed-to-mobile (F-to-M) cellular radio channels, Aulin [10] showed that the 2-D scattering models inaccurately predict the power spectral density and cross-correlation between antennas that are spatially separated in the vertical plane. Hence, our paper proposes a three-dimensional (3-D) theoretical model for outdoor MIMO M-to-M multipath fading channels. From the 3-D theoretical model, we derive a spatial correlation function for a 3-D non-isotropic scattering environment.

Antenna arrays hold an important role in designing bandwidth–efficient M-to-M systems. For most scattering environments, antenna spacing can have a significant effect on capacity and diversity. In this paper, using our 3-D spatial correlation function, we evaluate the effect of spatial correlation on the outage capacity of uniform linear antenna arrays (ULAs). The effects of antenna spacing and antenna orientations on the outage capacity are studied. Our results show that increasing distances between antenna elements in ULAs beyond 2λ has negligible effect on capacity. Furthermore, it is observed that when the radio propagation environment is characterized by 2-D isotropic scattering, orientations of the $\mathrm{T_x}$ and $\mathrm{R_x}$ antenna arrays in the x-y plane have no influence on capacity. This property of M-to-M channels is contrary to F-to-M channels, where broadside antenna arrays (array elements placed on the y-axis) provide higher capacity than the inline antenna arrays (array elements placed on the x-axis) [11]. When the outdoor radio propagation environment is characterized by 2-D non-isotropic scattering, the optimum capacity depends on the relative angle between the $\mathrm{T_x}$ ($\mathrm{R_x}$) antenna array and the orientation of local scatterers around the $\mathrm{T_x}$ ($\mathrm{R_x}$). Finally, our results show that if the available area in the x-y plane is insufficient for the antenna array realization, the antenna array can be tilted without a significant loss of capacity.

The remainder of the paper is organized as follows. Section II introduces a 3-D theoretical model for MIMO M-to-M channels and derives the corresponding spatial correlation function for a 3-D non-isotropic scattering environment. Section III evaluates effects of spatial correlation on the outage capacity of ULAs. Finally, Section IV provides some concluding remarks.

II. A 3-D Theoretical Model and Its Spatial Correlation Function

This paper considers a narrow-band MIMO communication system with L_t transmit and L_r receive omnidirectional antenna elements. It is assumed that both the $\mathrm{T_x}$ and $\mathrm{R_x}$ are in motion and equipped with low elevation antennas. The radio propagation environment is characterized by 3-D scattering with non-line-of-sight (NLoS) propagation conditions between the $\mathrm{T_x}$ and $\mathrm{R_x}$.

In this section, we introduce a 3-D theoretical model for outdoor MIMO M-to-M channels and derive its spatial correlation function. The starting point is a geometrical two-cylinder model for a MIMO M-to-M channel with $L_t = L_r = 2$ antenna elements shown in Fig. 1. The two-cylinder model is an extension of the one-cylinder model for F-to-M channels proposed in [10], [12]. By taking into account local scattering around both the $\mathrm{T_x}$ and $\mathrm{R_x}$ we obtain our two-cylinder model.

The two-cylinder model defines two cylinders, one around the $\mathrm{T_x}$ and another around the $\mathrm{R_x}$, as shown in Fig. 1. Around the transmitter, M fixed omnidirectional scatterers lie on a surface of a cylinder of radius R_t, and the m^{th} transmit scatterer is denoted by $S_T^{(m)}$. Similarly, around the receiver, N

0
Prepared through collaborative participation in the Collaborative Technology Alliance for Communications & Networks sponsored by the U.S. Army Research Laboratory under Cooperative Agreement DAAD19-01-2-0011. The U.S. Government is authorized to reproduce and distribute reprints for Government purposes notwithstanding any copyright notation thereon.

fixed omnidirectional scatterers lie on the surface of a cylinder of radius R_r, and the n^{th} receive scatterer is denoted by $S_R^{(n)}$. The distance between the centers of the $\mathrm{T_x}$ and $\mathrm{R_x}$ cylinders is D, and the spacing between antenna elements at the $\mathrm{T_x}$ and $\mathrm{R_x}$ is denoted by d_T and d_R, respectively. It is assumed that $\max\{d_T, d_R\} \ll \max\{R_t, R_r\} \ll D$. Angles θ_T and θ_R describe the orientation of the $\mathrm{T_x}$ and $\mathrm{R_x}$ antenna array in the x-y plane, respectively, relative to the x-axis. Similarly, angles ψ_T and ψ_R describe the elevation of the $\mathrm{T_x}$ and $\mathrm{R_x}$ antenna array relative to the x-y plane, respectively. The symbols $\alpha_T^{(m)}$ and $\alpha_R^{(n)}$ denote the azimuth angle of departure (AAoD) and the azimuth angle of arrival (AAoA), respectively. Similarly, the symbols $\beta_T^{(m)}$ and $\beta_R^{(n)}$ denote the elevation angle of departure (EAoD) and the elevation angle of arrival (EAoA), respectively. Finally, the symbols ϵ_{pm}, ϵ_{mn}, and ϵ_{nq} denote distances $A_T^{(p)}$–$S_T^{(m)}$, $S_T^{(m)}$–$S_R^{(n)}$, and $S_R^{(n)}$–$A_R^{(q)}$, respectively, as shown in Fig. 1.

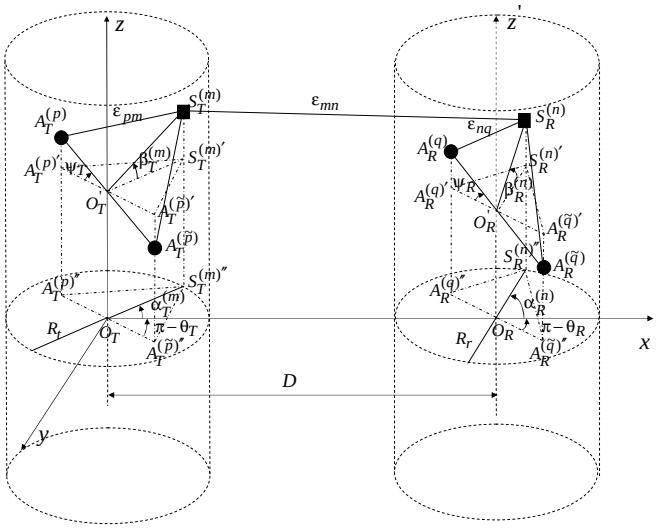

Fig. 1. The two-cylinder model for outdoor MIMO M-to-M channel with $L_t = L_r = 2$ antenna elements.

The received complex faded envelope of the link $A_T^{(p)} - A_R^{(q)}$ is

$$h_{pq} = \lim_{M,N\to\infty} \sqrt{\frac{1}{MN}} \sum_{m,n=1}^{M,N} e^{-j\frac{2\pi}{\lambda}(\epsilon_{pm}+\epsilon_{mn}+\epsilon_{nq})+j\phi_{mn}}, \quad (1)$$

where the ϕ_{mn} are random phases uniformly distributed on the interval $[-\pi, \pi)$ and λ is the carrier wavelength. The distances ϵ_{pm}, ϵ_{mn}, and ϵ_{nq} are, respectively,

$$\begin{aligned}
\epsilon_{pm} &\approx R_t - \frac{d_T(L_t+1-2p)}{2}\Big\{ \sin\psi_T \sin\beta_T^{(m)} \quad (2)\\
&- \cos\psi_T \cos\beta_T^{(m)} \left(\cos\theta_T \cos\alpha_T^{(m)} + \sin\theta_T \sin\alpha_T^{(m)}\right)\Big\},\\
\epsilon_{nq} &\approx R_r - \frac{d_R(L_r+1-2q)}{2}\Big\{ \sin\psi_R \sin\beta_R^{(n)} \quad (3)\\
&- \cos\psi_R \cos\beta_R^{(n)} \left(\cos\theta_R \cos\alpha_R^{(n)} + \sin\theta_R \sin\alpha_R^{(n)}\right)\Big\},\\
\epsilon_{mn} &\approx D. \quad (4)
\end{aligned}$$

Derivations of expressions (2) - (4) are omitted for brevity. Using (2) - (4), the complex faded envelope of the link $A_T^{(p)} - A_R^{(q)}$ can be rewritten as

$$h_{pq} = \lim_{M,N\to\infty} \frac{1}{\sqrt{MN}} \sum_{m,n=1}^{M,N} e^{j\phi_{mn}+j\phi_0} a_{p,m} b_{n,q}, \quad (5)$$

where $\phi_0 = -2\pi\left(R_t + R_r + D\right)/\lambda$ and parameters $a_{p,m}$ and $b_{n,q}$ are defined as

$$\begin{aligned}
a_{p,m} &= e^{j\frac{\pi}{\lambda}d_T(L_t+1-2p)\sin\psi_T \sin\beta_T^{(m)}} \times \quad (6)\\
&e^{j\frac{\pi}{\lambda}d_T(L_t+1-2p)\cos\psi_T \cos\beta_T^{(m)} \ \cos\theta_T \cos\alpha_T^{(m)} + \sin\theta_T \sin\alpha_T^{(m)}},\\
b_{n,q} &= e^{j\frac{\pi}{\lambda}d_R(L_r+1-2q)\sin\psi_R \sin\beta_R^{(n)}} \times \quad (7)\\
&e^{j\frac{\pi}{\lambda}d_R(L_r+1-2q)\cos\psi_R \cos\beta_R^{(n)} \ \cos\theta_R \cos\alpha_R^{(n)} + \sin\theta_R \sin\alpha_R^{(n)}}.
\end{aligned}$$

Assuming an outdoor 3-D non-isotropic scattering environment, we now derive the spatial correlation function of the complex faded envelope described in (5). The normalized spatial correlation function between two complex faded envelopes h_{pq} and $h_{\tilde{p}\tilde{q}}$ is defined as

$$R_{pq,\tilde{p}\tilde{q}}[d_T, d_R] = \frac{\mathrm{E}\left[h_{pq} h^*_{\tilde{p}\tilde{q}}\right]}{\sqrt{\mathrm{E}[|h_{pq}|^2]\mathrm{E}[|h_{\tilde{p}\tilde{q}}|^2]}}, \quad (8)$$

where $(\ \cdot\ )^*$ denotes complex conjugate operation, $\mathrm{E}[\ \cdot\ ]$ is the statistical expectation operator, $p, \tilde{p} \in \{1, \ldots L_t\}$, and $q, \tilde{q} \in \{1, \ldots L_r\}$. Using (5) and (8), the spatial correlation function can be written as

$$R_{pq,\tilde{p}\tilde{q}}[d_T, d_R] = \lim_{M,N\to\infty} \frac{1}{MN} \sum_{m,n=1}^{M,N} \mathrm{E}[a_{p,m} b_{n,q} a^*_{\tilde{p},m} b^*_{n,\tilde{q}}]. \quad (9)$$

Since the number of local scatterers in the the complex faded envelope in (5) is infinite, the discrete AAoDs, $\alpha_T^{(m)}$, EAoDs, $\beta_T^{(m)}$, AAoAs, $\alpha_R^{(n)}$, and EAoAs, $\beta_R^{(n)}$, can be replaced with continuous random variables α_T, β_T, α_R, and β_R with probability density functions (pdf) $f(\alpha_T)$, $f(\beta_T)$, $f(\alpha_R)$, and $f(\beta_R)$, respectively. To characterize the continuous random variables α_T and α_R, we use the von Mises pdf [13]

$$f(\theta) = \frac{1}{2\pi I_0(k)} \exp\left[k\cos(\theta - \mu)\right], \quad (10)$$

where $\theta \in [-\pi, \pi)$, $I_0(\ \cdot\ )$ is the zeroth-order modified Bessel function of the first kind, $\mu \in [-\pi, \pi)$ is the mean angle at which the scatterers are distributed in the x - y plane, and k controls the spread of scatterers around the mean. To characterize random variables β_T and β_R, we use the pdf [12]

$$f(\varphi) = \begin{cases} \frac{\pi}{4|\varphi_m|}\cos\left(\frac{\pi}{2}\frac{\varphi}{\varphi_m}\right) & , \ |\ \varphi\ | \leq |\ \varphi_m\ | \leq \frac{\pi}{2} \\ 0 & , \ \text{otherwise} \end{cases}, \quad (11)$$

where φ_m is the maximum elevation angle and takes values in the range $10^\circ \leq |\ \varphi_m\ | \leq 20^\circ$ [14]. It is assumed that the

angles of departure (α_T and β_T) and the angles of arrival (α_R and β_R) are random variables, and that the angles of departure are independent from the angles of arrival. The von Mises pdfs for the $\mathrm{T_x}$ and $\mathrm{R_x}$ azimuth angles are denoted as $f(\alpha_T) = \exp\left[k_T \cos(\alpha_T - \mu_T)\right]/(2\pi I_0(k_T))$ and $f(\alpha_R) = \exp\left[k_R \cos(\alpha_R - \mu_R)\right]/(2\pi I_0(k_R))$, respectively. The pdfs for the $\mathrm{T_x}$ and $\mathrm{R_x}$ elevation angles are denoted as $f(\beta_T) = \pi\cos(\pi\beta_T/(2\beta_{T_m}))/(4|\beta_{T_m}|)$ and $f(\beta_R) = \pi\cos(\pi\beta_R/(2\beta_{R_m}))/(4|\beta_{R_m}|)$, respectively. By grouping the terms in (9) into those containing α_T and β_T and those containing α_R and β_R, using trigonometric transformations, and applying the equality $\int_{-\pi}^{\pi} \exp\{a\sin(c) + b\cos(c)\}dc = 2\pi I_0\left(\sqrt{a^2+b^2}\right)$ [15, eq. 3.338-4], the spatial correlation function becomes

$$R_{pq,\tilde{p}\tilde{q}}[d_T, d_R] = R^T_{p,\tilde{p}}[d_T] R^R_{q,\tilde{q}}[d_R] = \quad (12)$$
$$\int_{-\beta_{T_m}}^{\beta_{T_m}} \pi\cos\left(\frac{\pi}{2}\frac{\beta_T}{\beta_{T_m}}\right) \frac{e^{j\frac{2\pi d_T(\tilde{p}-p)\sin\psi_T \sin\beta_T}{\lambda}} I_0\left(\sqrt{x^2+y^2}\cos\beta_T\right) d\beta_T}{4|\beta_{T_m}| I_0(k_T)}$$
$$\int_{-\beta_{R_m}}^{\beta_{R_m}} \pi\cos\left(\frac{\pi}{2}\frac{\beta_R}{\beta_{R_m}}\right) \frac{e^{j\frac{2\pi d_R(\tilde{q}-q)\sin\psi_R \sin\beta_R}{\lambda}} I_0\left(\sqrt{z^2+w^2}\cos\beta_R\right) d\beta_R}{4|\beta_{R_m}| I_0(k_R)},$$

where parameters x, y, z, and w are

$$\begin{aligned} x &\approx j2\pi d_T(\tilde{p}-p)\cos\theta_T\cos\psi_T/\lambda + k_T\cos\mu_T, \\ y &\approx j2\pi d_T(\tilde{p}-p)\sin\theta_T\cos\psi_T/\lambda + k_T\sin\mu_T, \quad (13) \\ z &\approx j2\pi d_R(\tilde{q}-q)\cos\theta_R\cos\psi_R/\lambda + k_R\cos\mu_R, \\ w &\approx j2\pi d_R(\tilde{q}-q)\sin\theta_R\cos\psi_R/\lambda + k_R\sin\mu_R. \end{aligned}$$

The integrals in (12) must be evaluated numerically, because they do not have closed-form solutions. Since β_T and β_R are small angles, i.e., $|\ \beta_T\ |, |\ \beta_R\ | \leq 20^\circ$, using approximations $\cos\beta_T, \cos\beta_R \approx 1$, $\sin\beta_T \approx \beta_T$, and $\sin\beta_R \approx \beta_R$, the spatial correlation function can be approximated as [16]

$$R_{pq,\tilde{p}\tilde{q}}[d_T, d_R] \approx \frac{I_0\left(\sqrt{x^2+y^2}\right)\cos\left(\frac{2\pi}{\lambda}\beta_{T_m} d_T(\tilde{p}-p)\sin\psi_T\right)}{I_0(k_T)\left[1 - \left(\frac{4\beta_{T_m} d_T(\tilde{p}-p)\sin\psi_T}{\lambda}\right)^2\right]}$$
$$\times \frac{I_0\left(\sqrt{w^2+z^2}\right)\cos\left(\frac{2\pi}{\lambda}\beta_{R_m} d_R(\tilde{q}-q)\sin\psi_R\right)}{I_0(k_R)\left[1 - \left(\frac{4\beta_{R_m} d_R(\tilde{q}-q)\sin\psi_R}{\lambda}\right)^2\right]}. \quad (14)$$

III. Effect of Spatial Correlation on the Outage Capacity of Uniform Linear Antenna Arrays

A. Review of MIMO Channel Capacity

The normalized channel capacity (in $\mathrm{bit/s/Hz}$) of a stochastic MIMO channel, under an average transmit power constraint, is given by [17]

$$C = \log_2 \det\left(\mathbf{I}_{L_r} + \frac{\rho}{L_t}\mathbf{H}\mathbf{H}^H\right), \quad (15)$$

where it is assumed that $L_t \geq L_r$, the transmitter has no channel knowledge, and the receiver has perfect channel knowledge. In (15), $\mathbf{H} = [h_{ij}]_{L_r \times L_t}$ is the matrix of the complex faded envelopes, $(\ \cdot\ )^H$ denotes the transpose conjugate operation, $\det(\ \cdot\ )$ denotes the matrix determinant, $\mathbf{I}_{L_r}$ is the $L_r \times L_r$ identity matrix, and ρ is the average signal-to-noise ratio (SNR). In the practice, the outage capacity is often used to characterize the properties of the MIMO channel. The outage capacity C_{out} is associated with an outage probability P_{out} which gives the probability that the channel capacity, C, falls below C_{out}.

The channel matrix $\mathbf{H}$ can be generated as a product of a white channel matrix and the square root of desired correlation matrices [17], i.e.,

$$\mathbf{H} = \left(\mathbf{R}_T[d_T]\right)^{1/2} \mathbf{G} \left(\mathbf{R}_R[d_R]\right)^{T/2}, \quad (16)$$

where $\mathbf{G}$ is an $L_t \times L_r$ stochastic matrix with complex Gaussian i.i.d. entries, $(\ \cdot\ )^{1/2}$ denotes the matrix square root operation, and $\mathbf{R}_T[d_T]$ and $\mathbf{R}_R[d_R]$ are the $L_t \times L_t$ transmit and the $L_r \times L_r$ receive spatial correlation matrix, respectively. The elements of matrices $\mathbf{R}_T[d_T]$ and $\mathbf{R}_R[d_R]$ are obtained using (14).

B. Simulation Results

In this section, the effect of spatial correlation on the outage capacity of uniform linear antenna arrays (ULAs) is investigated. In all simulations, we use a normalized sampling period $f_{T\max}T_s = 0.01$ ($f_{T\max} = f_{R\max}$ are the maximum Doppler frequencies and T_s is the sampling period) and calculate the outage capacity C_{out} for a 1% outage probability. Unless indicated otherwise, the following parameters are used: the maximum elevation angles are chosen to be $\beta_{T_m} = \beta_{R_m} = 15^\circ$; the SNR is set to 10 dB; the number of transmit and receive antennas is set to 3, i.e., $L_t = L_r = 3$ and the antenna arrays have $d_T = d_R = 1\lambda$; the orientations of the $\mathrm{T_x}$ and $\mathrm{R_x}$ antenna arrays are chosen to be $\theta_T = \theta_R = \pi/4$ and $\psi_T = \psi_R = \pi/3$; it is assumed that the local scatterers are centered around the x-axis, i.e., $\mu_T = 0^\circ$ and $\mu_R = 180^\circ$, and $k_T = k_R = 10$.

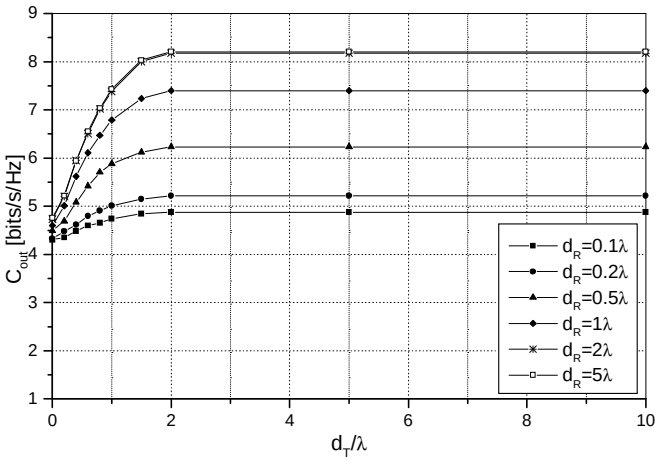

Fig. 2. Outage capacity as a function of spacing between the $\mathrm{T_x}$ and $\mathrm{R_x}$ antenna array elements.

Fig. 2 shows the outage capacity as a function of spacing between the $\mathrm{T_x}$ and $\mathrm{R_x}$ antenna array elements. We can observe that increasing antenna distances d_T and d_R up to

2λ increases the capacity from 4.3 bit/s/Hz to 8.2 bit/s/Hz. However, increasing antenna distances d_T and d_R beyond 2λ has negligible effect on the capacity.

For the $\mathrm{T_x}$ and $\mathrm{R_x}$ antenna arrays placed in the x - y plane, Fig. 3 shows the influence of the $\mathrm{T_x}$ and $\mathrm{R_x}$ antenna array orientations on the capacity. To analyze antenna array orientations only in the x - y plane, maximum elevation angles β_{T_m} and β_{R_m} are set to zero. From Fig. 3 we can observe that when 2-D isotropic scattering is assumed ($k_T = k_R = 0$), orientations of the $\mathrm{T_x}$ and $\mathrm{R_x}$ antenna arrays have no influence on the capacity. Note that this property of M-to-M channels is in contrast to F-to-M channels, where the broadside antenna arrays ($\theta_T = \theta_R = 90°$) provide higher capacity than the inline antenna arrays ($\theta_T = \theta_R = 0°$) [11]. When 2-D non-isotropic scattering is assumed ($k_T, k_R > 0$), Fig. 3 plots the outage capacity as a function of the $\mathrm{T_x}$ and $\mathrm{R_x}$ antenna array orientations for local scatterers centered around the x-axis, i.e., $\mu_T = 0°$ and $\mu_R = 180°$. We can observe that capacity

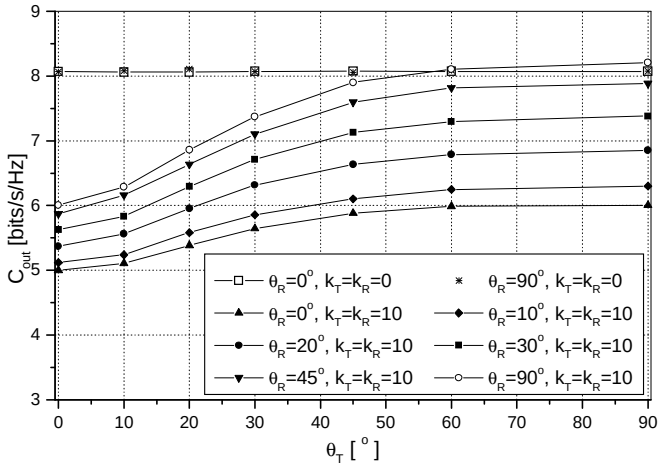

Fig. 3. Outage capacity as a function of the $\mathrm{T_x}$ and $\mathrm{R_x}$ antenna array orientations, θ_T and θ_R, for the local scatterers centered around the x-axis, i.e., $\mu_T = 0°$ and $\mu_R = 180°$.

is the lowest for inline antenna arrays ($\theta_T = \theta_R = 0°$) and the highest for broadside antenna arrays ($\theta_T = \theta_R = 90°$). Increasing antenna angles θ_T and θ_R from $0°$ to $45°$ increases capacity for 2.6 bit/s/Hz. However, further increase of antenna angles θ_T and θ_R from $45°$ to $90°$ increases capacity for only 0.6 bit/s/Hz. This implies that the optimum capacity will be obtain if angles θ_T and θ_R are between $45°$ and $90°$. However, if local scatterers are centered around the y-axis, (i.e., $\mu_T = 90°$ and $\mu_R = 270°$) capacity will be the lowest for broadside antenna arrays ($\theta_T = \theta_R = 90°$) and the highest for inline antenna arrays ($\theta_T = \theta_R = 0°$). This implies that the optimum capacity depends on the relative angle between the $\mathrm{T_x}$ antenna array and the local scatterers around the $\mathrm{T_x}$, i.e., $\mu_T - \theta_T$, and on the relative angle between the $\mathrm{R_x}$ antenna array and the local scatterers around the $\mathrm{R_x}$, i.e., $\mu_R - \theta_R$.

Figs. 4 and 5 show the influence of the $\mathrm{T_x}$ and $\mathrm{R_x}$ antenna elevation angles on the capacity. To study the influence of antenna elevation angles, we set angles θ_T and θ_R to $90°$ and

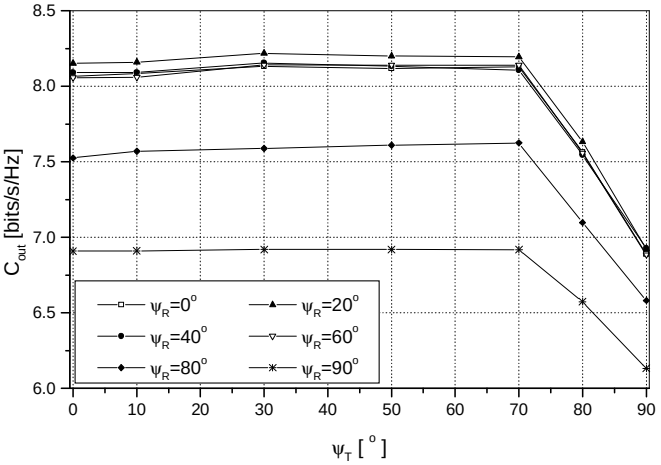

Fig. 4. Outage capacity as a function of the $\mathrm{T_x}$ and $\mathrm{R_x}$ antenna array elevations, ψ_T and ψ_R, for $k_T = k_R = 0$.

assume that local scatterers in the x - y plane are centered around the x-axis. From Fig. 3 we can observe that this selection of angles θ_T and θ_R will give us the highest capacity. In Fig. 4, the degree of local scattering in the x - y plane is $k_T = k_R = 0$. We can observe that increasing antenna angles ψ_T and ψ_R from $0°$ to $70°$ has small influence on the capacity. Further increase of antenna elevation angles drastically decreases the capacity. In Fig. 5, the degree of local

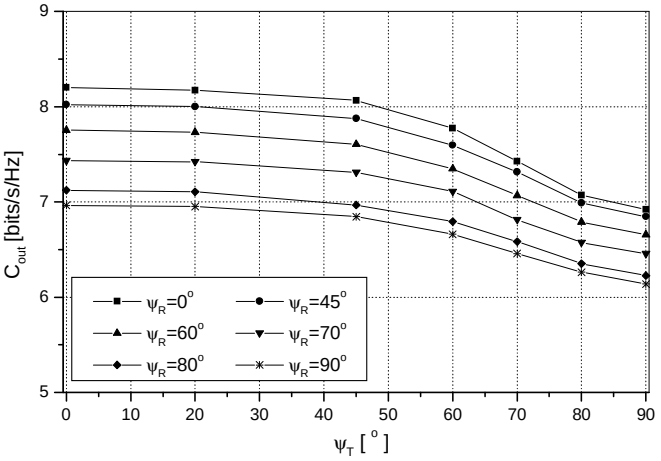

Fig. 5. Outage capacity as a function of the $\mathrm{T_x}$ and $\mathrm{R_x}$ antenna array elevations, ψ_T and ψ_R, for $k_T = k_R = 10$.

scattering in the x - y plane is increased to $k_T = k_R = 10$. By increasing antenna angles ψ_T and ψ_R from $0°$ to $45°$, the capacity decreases by only 0.3 bit/s/Hz. Further increase of antenna elevation angles drastically decreases the capacity. Figs. 4 and 5 imply that if available area in the x-y plane is not sufficient for realization, the antenna array can be tilted without significant loss of capacity. Finally, Figs. 6 and 7 study the effect of non-isotropic scattering on capacity. The orientations of the $\mathrm{T_x}$ and $\mathrm{R_x}$ antenna arrays are chosen to be $\theta_T = \theta_R = \pi/4$ and $\psi_T = \psi_R = \pi/4$. Fig. 6 shows how the capacity depends on the degree of local scattering in the

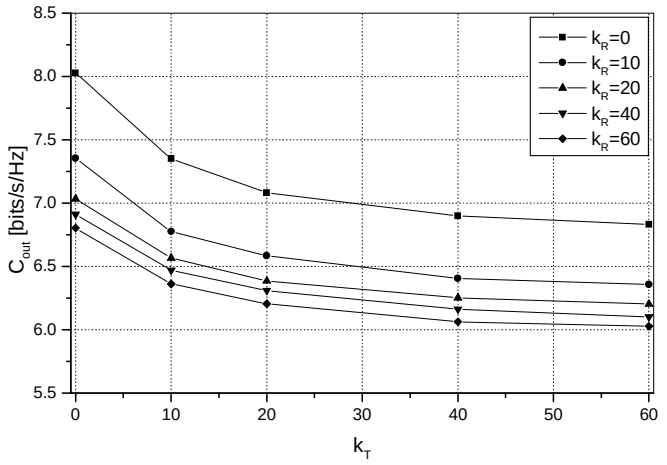

Fig. 6. Dependence of outage capacity on the degree of local scattering in the x - y plane, i.e., k_T, k_R.

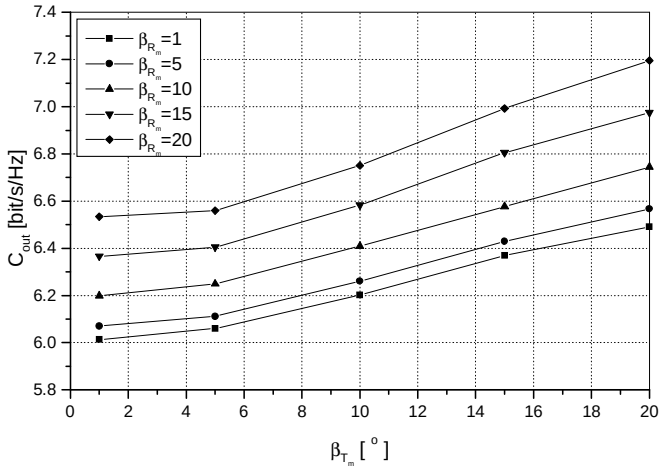

Fig. 7. Outage capacity as a function of the maximum elevation angles β_{T_m} and β_{R_m}.

x - y plane, i.e., k_T and k_R. As the parameters k_T and k_R increase, the scattering in the x-y plane becomes more non-isotropic, leading to lower capacity. Fig. 7 shows the capacity as a function of the maximum elevation angles β_{T_m} and β_{R_m}. We can observe that by increasing maximum elevation angles β_{T_m} and β_{R_m} from 1° to 20° the capacity increases up to 1 bit/s/Hz. This result implies that the 2-D models underestimate available capacity by up to 1.2 bit/s/Hz.

IV. Conclusions

In this paper, a 3-D theoretical model for outdoor MIMO M-to-M fading channels is proposed and its spatial correlation function is derived. Using this correlation function, the effect of space-time correlation on the outage capacity of ULAs is evaluated. The results show that increasing distance between antenna elements in ULAs beyond 2λ has negligible effect on the capacity. Furthermore, when the radio propagation environment is characterized by 2-D isotropic scattering, orientations of the $\mathrm{T_x}$ and $\mathrm{R_x}$ antenna arrays in the x-y plane have no influence on the capacity. When the radio propagation environment is characterized by 2-D non-isotropic scattering, the optimum capacity depends on the relative angle between the $\mathrm{T_x}$ ($\mathrm{R_x}$) antenna array and the orientation of local scatterers around the $\mathrm{T_x}$ ($\mathrm{R_x}$). Finally, the results show that if available area in the x-y plane is not sufficient for the antenna array realization, the antenna array can be tilted without significant loss of capacity.

Disclaimer

The views and conclusions contained in this document are those of the authors and should not be interpreted as representing the official policies, either expressed or implied, of the Army Research Laboratory or the U. S. Government.

References

[1] A.S. Akki and F. Haber, "A statistical model for mobile-to-mobile land communication channel," *IEEE Trans. on Veh. Tech.*, vol. 35, pp. 2–10, Feb. 1986.

[2] A.S. Akki, "Statistical properties of mobile-to-mobile land communication channels," *IEEE Trans. on Veh. Tech.*, vol. 43, pp. 826–831, Nov. 1994.

[3] R. Wang and D. Cox, "Channel modeling for ad hoc mobile wireless networks," *Proc. IEEE Veh. Tech. Conf.*, vol. 1, pp. 21–25, Birmingham, AL, May 2002.

[4] C.S. Patel, G.L. Stüber, and T. G. Pratt, "Simulation of Rayleigh-faded mobile-to-mobile communication channels," *IEEE Trans. on Commun.*, vol. 53, pp. 1876–1884, Nov. 2005.

[5] A.G. Zajić and G.L. Stüber, "A new simulation model for mobile-to-mobile Rayleigh fading channels," *Proc. IEEE WCNC'06*, vol. 3, pp. 1266–1270, Las Vegas, NE, USA, Apr. 2006.

[6] M. Pätzold, B.O. Hogstad, N. Youssef, and D. Kim, "A MIMO mobile-to-mobile channel model: part I - the reference model," *Proc. IEEE PIMRC'05*, vol. 1, pp. 573–578, Berlin, Germany, Sept. 2005.

[7] A.G. Zajić and G.L. Stüber, "Space-Time Correlated MIMO Mobile-to-Mobile Channels," *Proc. IEEE PIMRC'06*, Helsinki, Finland, Sept. 2006.

[8] B.O. Hogstad, M. Pätzold, N. Youssef, and D. Kim, "A MIMO mobile-to-mobile channel model: part II - the simulation model," *Proc. IEEE PIMRC'05*, vol. 1, pp. 562–567, Berlin, Germany, Sept. 2005.

[9] A.G. Zajić and G.L. Stüber, "Simulation Models for MIMO Mobile-to-Mobile Channels," *Proc. IEEE MILCOM'06*, Washington, D.C., USA, Oct. 2006.

[10] T. Aulin, "A modified model for the fading at a mobile radio channel," *IEEE Trans. on Veh. Tech.*, vol. VT–28, pp. 182–203, 1979.

[11] D. Shiu, G.J. Foschini, M.J. Gans, and J.M. Khan, "Fading correlation and its effect on the capacity of multielement antenna systems," *IEEE Trans. on Commun.*, vol. 48, pp. 502–513, Mar. 2000.

[12] J.D. Parsons and A.M.D. Turkmani, "Characterisation of mobile radio signals: model description," *IEE Proc. I, Commun., Speach, and Vision*, vol. 138, pp. 549–556, Dec. 1991.

[13] A. Abdi, J.A. Barger, and M. Kaveh, "A parametric model for the distribution of the angle of arrival and the associated correlation function and power spectrum at the mobile station," *IEEE Trans. on Veh. Tech.*, vol. 51, pp. 425–434, May 2002.

[14] Y. Yamada, Y. Ebine, and N. Nakajima, "Base station/vehicular antenna design techniques employed in high capacity land mobile communications system," *Rev. Elec. Commun. Lab.*, NTT, pp. 115–121, 1987.

[15] I.S. Gradshteyn and I.M. Ryzhik, *Table of Integrals, Series, and Products* 5^{th} *ed.*. A. Jeffrey, Ed. San Diego CA: Academic, 1994.

[16] A.G. Zajić and G.L. Stüber, "A three-dimensional MIMO mobile-to-mobile channel model," to appear in *IEEE WCNC'07*, Hong Kong, March 2007.

[17] D. Gesbert, H. Bölcskei, D.A. Gore, and A.J. Paulraj, "Outdoor MIMO wireless channels: models and performance prediction," *IEEE Trans. on Commun.*, vol. 50, pp. 1926–1934, Dec. 2002.

[18] G. L. Stüber, *Principles of mobile communication 2e.*Kluwer, 2001.